

AINTEGUMENTA-LIKE6 regulates cellular differentiation in flowers

Beth A. Krizek · Marcie Eaddy

Received: 7 May 2011 / Accepted: 29 October 2011 / Published online: 11 November 2011
© Springer Science+Business Media B.V. 2011

Abstract During flower development, pluripotent stem cells within the floral meristem give rise to proliferative precursor cells whose progeny eventually acquire specialized functions within each floral organ. The regulatory mechanisms by which plant cells transition from a proliferating state to a differentiated state are not well characterized. Several members of the *AINTEGUMENTA-LIKE/PLETHORA* (*AIL/PLT*) transcription factor family, including *AINTEGUMENTA* (*ANT*) and *AIL6/PLT3*, are important regulators of cell proliferation in flowers. To further investigate the role of *AIL6* during flower development, we have characterized transgenic plants in which the coding region of *AIL6* was expressed under the control of the constitutive *35S* promoter (*35S:cAIL6*). These plants display changes in floral organ size and morphology that are associated with alterations in the pattern and duration of cell divisions within developing organs. In addition, we find that very high levels of *AIL6* expression inhibit cellular differentiation. In contrast, *ant ail6* double mutants display premature differentiation of floral meristem cells. These results indicate that these two transcription factors regulate both proliferation and differentiation in flowers.

Keywords *Arabidopsis* · Flower development · Differentiation · *AP2/ERF* · *AIL/PLT* · Organogenesis

Introduction

During reproductive development in *Arabidopsis thaliana*, pluripotent stem cells within the floral meristem give rise to

highly proliferative progeny cells which transition through various stages of differentiation before becoming fully differentiated and ceasing cell division. The exact mechanisms controlling the transition of cells within developing floral organ primordia from a proliferating state to a differentiated state and how they are integrated within the programs of floral organ identity specification are not well understood. Floral organ primordia adopt distinct fates in response to the activities of unique combinations of floral organ identity proteins [reviewed in (Irish 2010)]. These proteins appear to regulate the entire process of floral organogenesis, from the progressive elaboration of organ morphology to cell and tissue-type patterning [reviewed in (Sablowski 2010; Ito 2011)].

According to the ABCE model, four different classes of floral organ identity proteins act in different combinations to specify sepal, petal, stamen and carpel identity in whorls one to four of the flower, respectively [reviewed in (Krizek and Fletcher 2005)]. The combination of A and E gene activities specifies sepal identity, the combination of A, B and E activities specifies petal identity, the combination of B, C and E activities specifies stamen identity and the combination of C and E activities specifies carpel identity. With the exception of the class A protein *APETALA2* (*AP2*), the remaining floral organ identity proteins [the class A protein *APETALA1* (*AP1*), the class B proteins *APETALA3* (*AP3*) and *PISTILLATA* (*PI*), the class C protein *AGAMOUS* (*AG*), and the class E *SEPALATA* (*SEP*) proteins] are MADS domain transcription factors. According to the quartet model, these MADS domain proteins form higher order protein complexes, likely tetramers, that bind to $CC(A/T)_6GG$ (CArG boxes) sequences in the promoters of target genes (Theissen 2001; Melzer and Theissen 2009; Melzer et al. 2009). The floral organ identity proteins regulate distinct genes at different times in

B. A. Krizek (✉) · M. Eaddy
Department of Biological Sciences, University of South
Carolina, Columbia, SC 29208, USA
e-mail: krizek@sc.edu

flower development with identified targets including genes involved in hormonal pathways, growth control and patterning (Kaufmann et al. 2009, 2010).

A number of genes regulating floral organ growth in *Arabidopsis* have been identified with some genes primarily controlling cell proliferation and others cell elongation [reviewed in (Breuninger and Lenhard 2010)]. Promoters of organ growth that regulate cell division include *AINTEGUMENTA* (*ANT*) and *AINTEGUMENTA-LIKE6/PLETHORA3* (*AIL6/PLT3*), two members of the *AIL/PLT* gene family that encode AP2/ERF type transcription factors. *ant* mutants produce smaller leaves and flowers than wild type and these organ growth defects are enhanced in *ant ail6* double mutants (Elliott et al. 1996; Klucher et al. 1996; Krizek 2009). Both genes are expressed throughout the floral meristem and newly initiated floral organ primordia, but *ANT* expression persists longer than that of *AIL6* in developing floral organs with little or no expression in mature organs (Elliott et al. 1996; Nole-Wilson et al. 2005). *ANT* has been proposed to regulate organ size by controlling the length of time in which cells within developing organs are competent to undergo proliferation (Mizukami and Fischer 2000). Constitutive expression of *ANT* under the 35S promoter resulted in persistent expression of the G1 cyclin *CycD3* in maturing leaves, a prolonged period of cell division and larger organs (Mizukami and Fischer 2000).

Besides its role in regulating organ growth in the shoot, *AIL6/PLT3* acts redundantly with *PLT1* and *PLT2* in root development (Galinha et al. 2007). *plt1plt2 ail6* seedlings have a rootless phenotype with fully differentiated cells present in the root pole of these seedlings at 3 days post germination (Galinha et al. 2007). Four *AIL/PLT* proteins (*PLT1*, *PLT2*, *AIL6* and *BBM*) are detected in gradients within the root with the highest levels present in the stem cell niche and lower levels in the proliferating cells above the meristem (Galinha et al. 2007). Low levels of *PLT2* and *PLT3* are also detected in cells of the elongation zone. This gradient of *PLT* activity has been proposed to be instructive for distinct cellular behaviors with high *PLT* activity specifying stem cell identity, intermediate levels specifying mitotic activity and low levels required for cellular differentiation (Galinha et al. 2007).

To further investigate the role of *AIL6* during flower development, we expressed the coding region of *AIL6* under the control of the constitutive 35S promoter (*35S:cAIL6*). These plants exhibit alterations in floral organ morphology that are associated with persistent cell divisions within some developing floral organs. The severity of these phenotypic alterations is correlated with *AIL6* mRNA levels. In the highest expressing *35S:cAIL6* line characterized, we also observed negative effects on cellular differentiation. The characteristic surface morphologies of

sepal, petal, stamen and carpel epidermal cells were absent in this *35S:cAIL6* line suggesting that cells did not undergo complete differentiation. Correspondingly, we observe that floral meristem cells undergo premature differentiation in *ant ail6* flowers. These findings suggest that *ANT* and *AIL6* regulate the transition of cells between proliferation and differentiation.

Materials and methods

Plant materials and growth conditions

Arabidopsis thaliana ecotype Landsberg *erecta* (*Ler*) was used as the wild type. Plants were grown on a soil mixture of Metro-Mix 360:perlite:vermiculite (5:1:1) under continuous light or in 16 h days (100–150 $\mu\text{mol}/\text{m}^2/\text{s}$) at a temperature of 22°C.

Plasmid construction and *Agrobacterium* transformation

The coding region of *AIL6* (*cAIL6*), corresponding to the most upstream in-frame ATG (Feng et al. 2005), was PCR amplified from cDNA and cloned into the KpnI/BamHI sites of pART7. The resulting *35S:cAIL6* construct was digested with NotI and cloned into pMLBart. The *35S:cAIL6* plasmid was transformed into *Agrobacterium tumefaciens* strain ASE by electroporation. *Arabidopsis Ler* plants were transformed with this *Agrobacterium* strain by vacuum infiltration (Bechtold et al. 1993). Transformants containing the *35S:cAIL6* transgene were selected using basta.

RNA extraction and real time RT-PCR

RNA was extracted from inflorescences (Verwoerd et al. 1989) and treated with Turbo DNase (Applied Biosystems) following the manufacturer's instructions. First strand cDNA synthesis was performed using Quanta qScript cDNA Super Mix (Quanta BioSciences) following the manufacturer's instructions. The real time PCR reactions were performed on an iCycler (Biorad) using B-R SYBR Green SuperMix for iQ (Quanta BioSciences) and the following primers for *AIL6*: RTAIL6-4: 5'-cgagttgctggaacaaag-3' and RTAIL6-5: 5'-tcatacgettcagctgcttc-3', which amplified a 71 bp fragment. Melt curve analyses were performed at the end of each experiment to check the specificity of the reactions. Experiments were performed twice using two or three biological tissue replicates and reactions in triplicate. The raw fluorescence data was analyzed using Miner, a software program that calculates Ct (threshold cycle) and amplification efficiencies (Zhao and Fernald 2005). Normalization was performed using

two reference genes (At5g15710, At5g12240) that are expressed stably and at lower levels than traditional reference genes, since *AIL6* expression is low (Czechowski et al. 2005). The fold difference in *AIL6* expression was calculated using the Pfaffl method (Pfaffl 2001). Data reported in the figures correspond to those normalized to At5g12240 but similar values were obtained when normalizing to At5g15710.

SEM

Tissue for SEM was fixed, dried, dissected and coated as described previously (Krizek 1999). SEM analyses were performed on a FEI Quanta 200 ESEM.

Paraffin and epoxy sectioning

Tissue for paraffin sectioning was prepared and sectioned as described below for in situ hybridization. After sectioning, slides were placed in 0.05% Toluidine Blue O for 10 min, rinsed with water and allowed to air dry (Sakai 1973). The paraffin was removed with xylenes and slides mounted with permount. For embedding in epoxy, tissue was fixed in 0.2 M sodium cacodylate buffer for 2 h at room temperature, rinsed with 0.1 M cacodylate buffer, postfixed in 0.1 M cacodylate buffered 1% osmium tetroxide for 1 h at 4°C, rinsed with 0.1 M cacodylate buffer, dehydrated in ethanol and acetone, and incubated overnight in a 1:1 mixture of EMBed-812 (Electron Microscopy Sciences) and acetone. The next day the tissue was incubated for 5 h in a 3:1 mixture of EMBed-812 and acetone and then incubated overnight in 100% EMBed-812. The samples were embedded the next day in 100% EMBed-812 and cured for approximately 24 h. Samples were sectioned on an ultramicrotome and stained with Toluidine Blue O (Epoxy tissue stain; Electron Microscopy Sciences).

In situ hybridization

Inflorescences were fixed, embedded, sectioned, hybridized and washed as described previously (Krizek 1999). Digoxigenin-labeled antisense RNA probes (*AIL6*, *histone H4*) were synthesized as described previously (Krizek 1999; Nole-Wilson et al. 2005).

Results

35S:cAIL6 plants exhibit alterations in floral organ development

To better understand the role of *AIL6* in plant development, the coding region of *AIL6* was expressed under the control

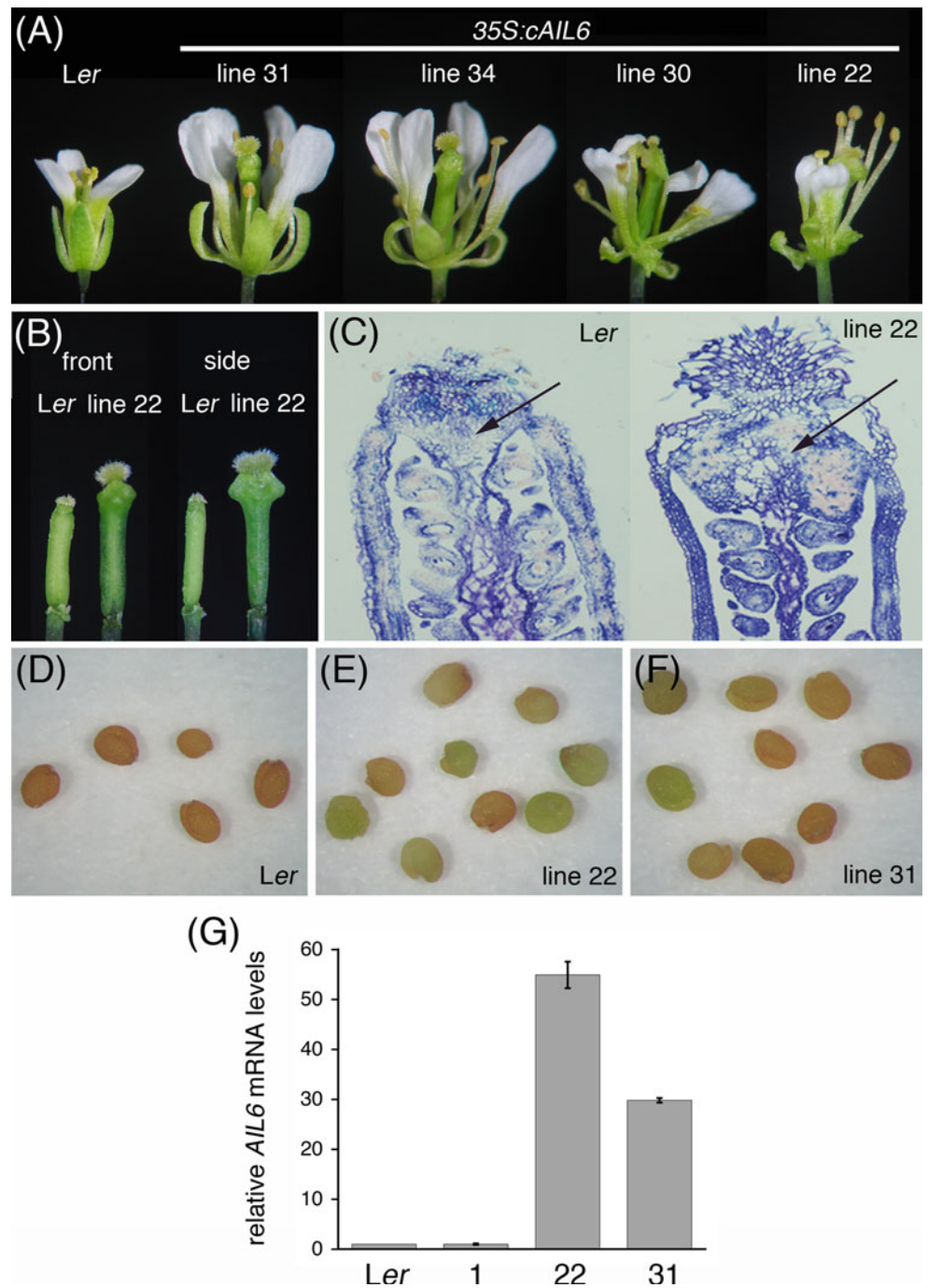
of the constitutive *35S* promoter from the cauliflower mosaic virus. The majority of T1 plants (75 lines) exhibited alterations in flower development while 20 lines had a wild-type appearance. The alterations in flower development included changes in floral organ size and morphology (Fig. 1a). Most T1 lines were infertile, but we were able to obtain seeds from several lines. We chose two lines with phenotypes, lines 22 and 31, for further phenotypic characterization. These lines had partially overlapping but somewhat distinct phenotypes.

Flowers of line 22 sometimes produce floral organs larger than wild type but more often display dramatic changes in organ morphology (Fig. 1a). The severity of these morphological changes varies somewhat between plants and between flowers on a single plant with the most variation observed in the sepal and petal phenotypes. In the most severe cases, the sepals are bent backwards, cupped and bumpy with a fringe-like appearance at their distal end (Fig. 2a, b). Because of their altered morphology, they do not fully enclose the floral bud. Petals are cupped and sometimes fringed at their distal end (Fig. 2c). The anthers of stamens are somewhat misshapen with less clearly defined locules, many of which do not release pollen (Fig. 2d). The floral organs that differ most dramatically from wild type are the carpels, which have large outgrowths in the styler region of the organ (Fig. 1b). These carpel outgrowths are most dramatic in the medial domain (corresponding to the region of fusion of the two carpels) but smaller bumpy protrusions are also detected in the lateral region (Figs. 1b, 2e–h). Sections through the gynoecium show increased numbers of cells in the styler region of the *35S:cAIL6* line 22 carpels compared to wild-type carpels (Fig. 1c). Flowers of line 31 produce larger floral organs that are generally similar in overall appearance to those of wild type (Fig. 1a). However, the sepals of these flowers are more cupped in shape than in wild type and the carpels have similar but somewhat less dramatic protrusions as described for line 22.

Some later-arising flowers in both *35S:cAIL6* line 22 and 31 have a more normal appearance and are fertile, allowing us to obtain some seeds from these lines. The seeds obtained are sometimes larger than normal with light brown or greenish seed coats that never take on the brown color of wild-type mature seeds (Fig. 1d–f). The seed phenotype, like the flower phenotype, is more severe in line 22 compared to line 31.

To determine whether the phenotypic differences between lines 22 and 31 might be a consequence of different steady-state levels of *AIL6* mRNA, we characterized *AIL6* expression in three *35S:cAIL6* lines (1, 22, 31) and wild type inflorescences by real-time RT-PCR. *35S:cAIL6* line 1 produces flowers with a wild-type appearance and accumulates similar amounts of *AIL6* mRNA as wild-type

Fig. 1 *AIL6* misexpression alters flower and seed development. **a** Flowers from wild type (*Ler*) and *35S:cAIL6* lines 31, 34, 30 and 22 showing phenotypic variation from primarily effects on organ size to dramatic changes in organ morphology (*left to right*). **b** Front (replum up) and side (replum on side) views of mature *Ler* and *35S:cAIL6* line 22 carpels. **c** Sections of paraffin-embedded tissue showing the apical region of mature *Ler* and *35S:cAIL6* line 22 carpels. *Arrows* point to the stylar region, which undergoes increased proliferation in *35S:cAIL6* line 22. Seeds from *Ler* (**d**), *35S:cAIL6* line 22 (**e**) and *35S:cAIL6* line 31 (**f**). *AIL6* mRNA levels in *Ler* and *35S:cAIL6* (lines 1, 22, and 31) inflorescences. The expression level in *Ler* is set to one and *error bars* show standard deviation



inflorescences (Fig. 1g). In contrast, *AIL6* mRNA levels were much higher in lines 22 and 31 as compared with wild type. *AIL6* mRNA levels were approximately 55 fold higher in line 22 and approximately 30 fold higher in line 31 (Fig. 1g). These results suggest that the stronger floral and seed phenotypes of line 22 are a consequence of higher levels of *AIL6* mRNA.

To better characterize the altered morphology of *35S:cAIL6* line 22 carpels, we examined these organs

throughout flower development by scanning electron microscopy. In stage 11 and younger flowers, *35S:cAIL6* carpels appear normal in morphology (Fig. 2i, j). During stage 12 of wild-type flower development, stigmatic papillae appear at the apex of the carpel and the stylar region become clearly distinct from the stigma above and the ovary valves below (Fig. 2k). In *35S:cAIL6* flowers, the stylar region is tapered but not as well-defined and distinct from the ovary valve tissue (Fig. 2l). This continues to be

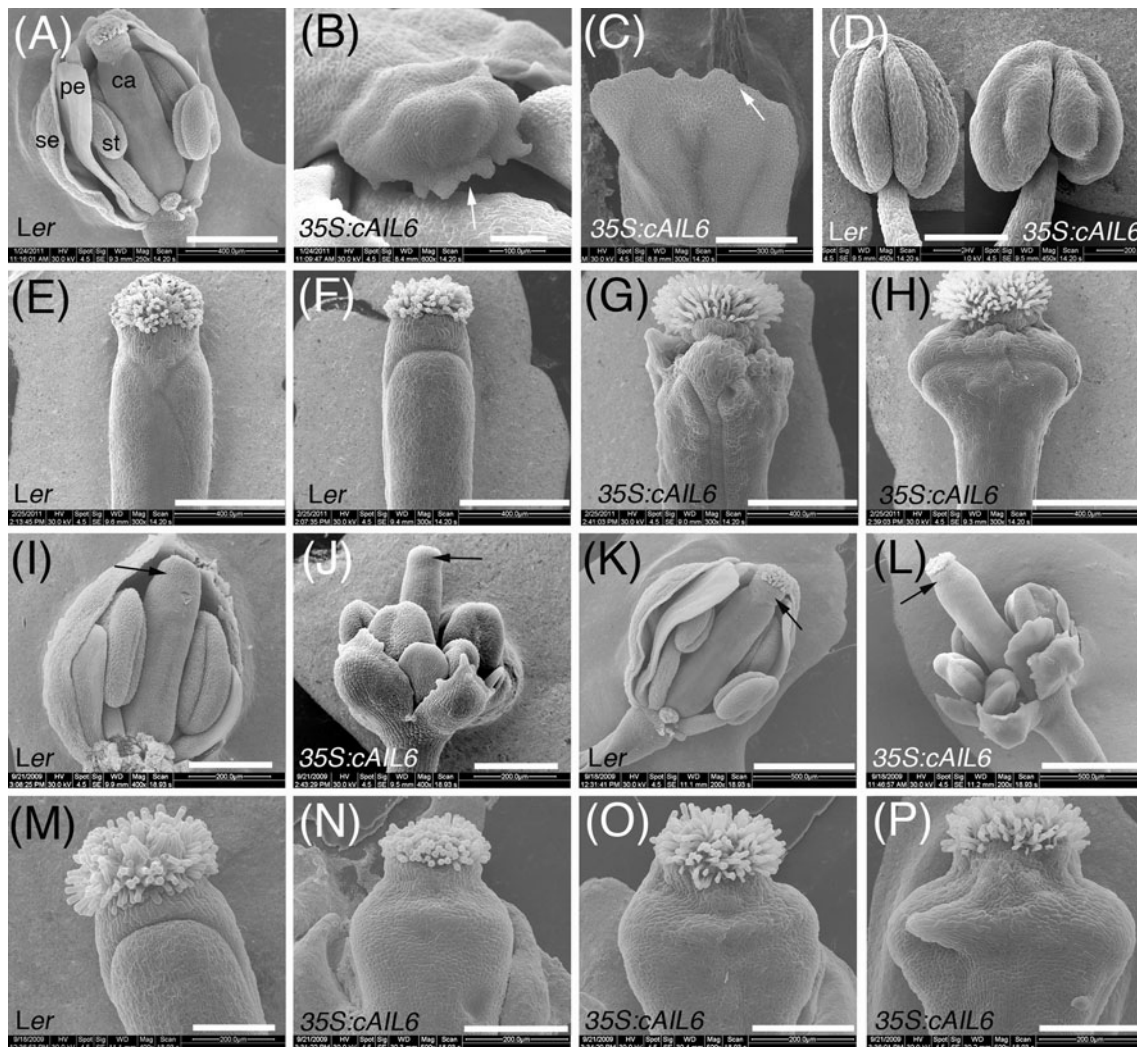


Fig. 2 SEM analyses of *35S:cAIL6* line 22 floral organs. **a** *Ler* flower. **b** *35S:cAIL6* sepal with a bumpy appearance. *Arrow* points to fringe present at the distal end of the sepal. **c** *35S:cAIL6* petal with fringe at the distal end (*arrow*). **d** *Ler* (*left*) and *35S:cAIL6* (*right*) stamen anthers. **e** Front view (replum up) of *Ler* carpel. **f** Side view (replum to side) of *Ler* carpel. **g** Front view of *35S:cAIL6* carpel showing small bumpy protrusions below the stigma. **h** Side view of *35S:cAIL6* carpel showing large extensions beneath the stigma. **i** *Ler* flower of stage 10. *Arrow* points to the top of the carpel. **j** *35S:cAIL6*

flower of stage 10. *Arrow* points to the *top* of the carpel that has a normal appearance at this stage of development. **k** *Ler* flower of stage 12. *Arrow* points to style. **l** *35S:cAIL6* flower of stage 12. Style (*arrow*) is not as distinctly separated from the ovary valves as in wild type. **m** Closeup view of side view of *Ler* carpel. **n–p** Developmental series showing the progressive enlargement of the carpel outgrowths of *35S:cAIL6* flowers. *SE* sepal, *PE* petal, *ST* stamen, *CA* carpel. Size bars are 100 μ M (**b**), 200 μ M in (**c**, **d**, **i**, **j**, **m–p**), 400 μ M in (**a**, **e–h**) and 500 μ M (**k**, **l**)

true through opening of the floral bud in stage 13 flowers. Bulging from the stylar region begins to occur in *35S:cAIL6* line 22 carpels during stage 13 and continues with the bulges developing into larger outgrowths (Fig. 2m–p).

Dosage dependent effects of *AIL6* misexpression on cellular differentiation in floral organs

Each of the four floral organs exhibits distinct and characteristic epidermal cell morphologies at maturity (Fig. 3a–d). The abaxial surface of sepals contains cells of variable

size with characteristic cuticular thickenings (Fig. 3a). The adaxial petal surface consists of conical shaped cells with cuticular markings running down from the cell apex (Fig. 3b). Anther cells are interdigitated and also display characteristic cuticular thickenings (Fig. 3c) while ovary valve epidermal cells have specks of epicuticular wax on their surface (Fig. 3d). Epidermal cells present on *35S:cAIL6* line 22 floral organs lack these characteristic features of differentiated floral organs. The epidermal cells present on sepals, petals and stamens are smooth in appearance, lacking the cuticular thickenings (Fig. 3e–g), and epicuticular wax was not present on ovary valve cells

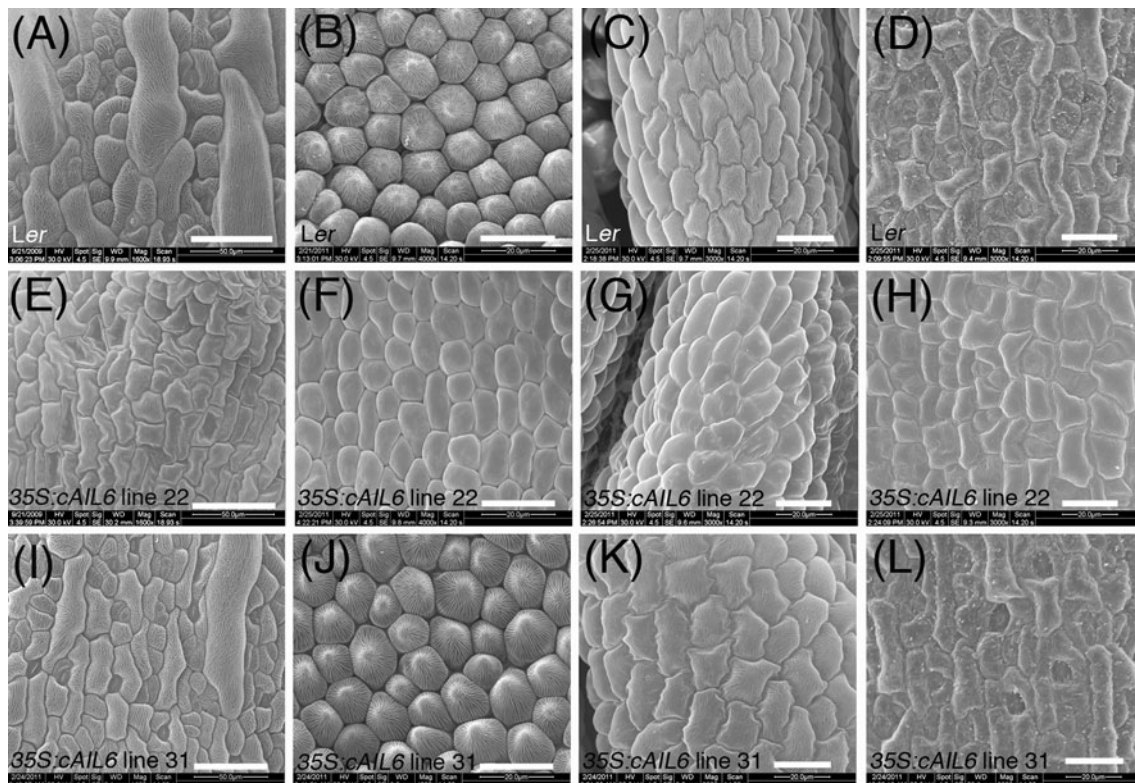


Fig. 3 SEM analyses of epidermal surface of *35S:cAIL6* floral organs. Epidermal surface of *Ler* sepal (a), petal (b), anther (c) and ovary valve (d). Epidermal surface *35S:cAIL6* line 22 sepal (e), petal (f), anther (g) and ovary valve (h). These cells lack the characteristic cuticular markings present on the corresponding *Ler* cells and

sometimes have an altered shape. Epidermal surface *35S:cAIL6* line 31 sepal (i), petal (j), anther (k) and carpel valve (l). These cells possess the characteristic cuticular markings present on the corresponding *Ler* cells. Size bars are 50 μ m (a–l)

(Fig. 3h). In addition cell size and shape was sometimes altered. No giant cells were present on the sepal abaxial epidermis (Fig. 3e). Some adaxial petal epidermal cells were more elongated (Fig. 3f) and anther cells were less interdigitated (Fig. 3g). The altered cell shape and epidermal characteristics were somewhat variable; ranging from some organs with normal epidermal characteristics to those with a few normal cells in a background of mostly cells with smooth appearances to organs that only contained organs with smooth cells. These cellular phenotypes were correlated with overall organ morphology; organs most dramatically affected in overall appearance displayed the most dramatic differences at the cellular level. No alterations in epidermal cell surface morphology or cell shape were ever observed in *35S:cAIL6* line 31 floral organs (Fig. 3i–l).

To further investigate whether *AIL6* regulates cell differentiation, we examined epoxy-embedded sections of *ant ail6* inflorescences since *ail6* mutants have a wild-type appearance. The sections were stained with Toluidine Blue O, a polychromatic stain that differentially stains different cellular components (O'Brien et al. 1964; Sakai 1973). The inflorescence meristem and stage 1–3 flowers of *Ler* and

ant ail6 inflorescences are similar in appearance with both inflorescence and floral meristems composed of small and densely staining cells filled with cytoplasm (Fig. 4a, d). Floral meristem cells in stage 5 wild-type flowers also exhibit dense staining (Fig. 4b), while cells in the floral meristem region of similar stage *ant ail6* flowers are less densely staining with larger vacuoles (Fig. 4e). While young stamen and carpel primordia in wild-type flowers stain darkly (Fig. 4c), this is not true of primordia that arise in the center of *ant ail6* flowers (Fig. 4f). Thus in the absence of *ANT* and *AIL6* function, floral meristem cells undergo premature differentiation, which could be at least partly responsible for the reduced size of *ant ail6* floral organs (Krizek 2009).

AIL6 overexpression does not affect leaf development

In addition to their altered appearance, many *35S:cAIL6* seeds exhibited delayed germination such that seedling size was quite variable 7 days after transfer of seeds on plates into the growth room (Fig. 5a–c). This phenotype was stronger in line 22 compared with line 31. *AIL6* overexpression does not affect vegetative development as

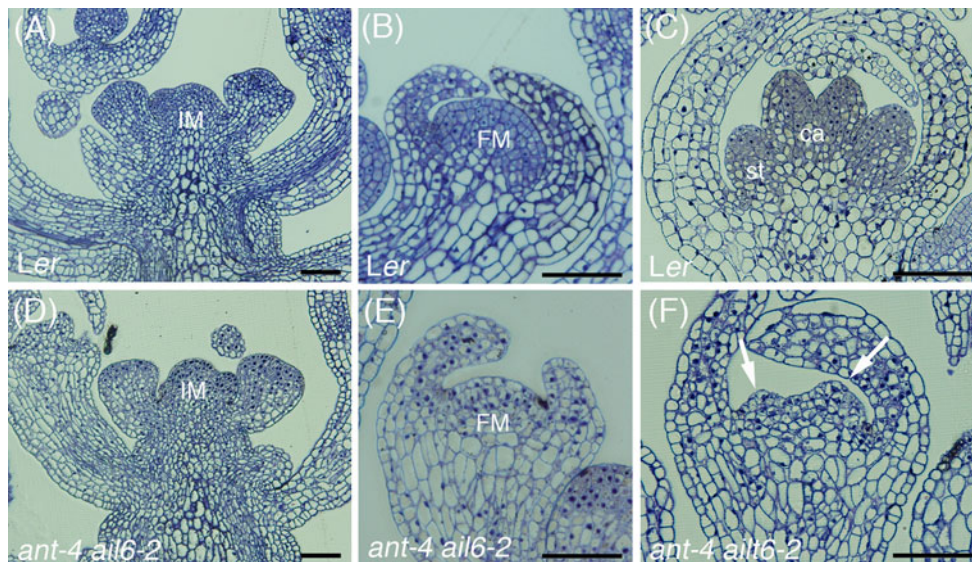


Fig. 4 *ant ail6* flowers show premature differentiation of floral meristem cells. Thin epoxy sections of *Ler* inflorescence (a), stage 5 flower (b) and stage 7 flower (c). The floral meristem (FM) consists of small densely stained cells. In c, stamen (st) and carpel (ca) primordia consist primarily of small densely stained cells. Thin sections of *ant-4 ail6-2*

ail6-2 inflorescence (d), stage 5 flower (e) and stage 6 flower (f). Cells in the floral meristem (e) or within organ primordia (f) are larger, less densely stained with large vacuoles compared to those in *Ler*. IM inflorance meristem, FM floral meristem, ST stamen, CA carpel. Size bars correspond to 50 μ m (a–f)

35S:cAIL6 plants are normal in appearance approximately 17 days after germination (Fig. 5d–f) and bolt at the same time as wild type (Fig. 5g). Because of the normal appearance of these plants, we measured steady-state *AIL6* mRNA levels in 20 day old shoots. Both *35S:cAIL6* lines 22 and 31 had greatly increased levels of *AIL6* transcript with line 22 exhibiting almost 70 fold and line 31 approximately 50 fold more *AIL6* mRNA than wild type (Fig. 5h). We also examined the surface morphology of rosette leaves and found no differences in the epidermal cellular characteristics of *35S:cAIL6* leaves line 22 or 31 as compared with *Ler* leaves (Fig. 5i–k). These results indicate that high levels of *AIL6* mRNA do not affect vegetative development or the switch to reproductive development.

Persistent cell division is associated with the altered development of *35S:cAIL6* floral organs

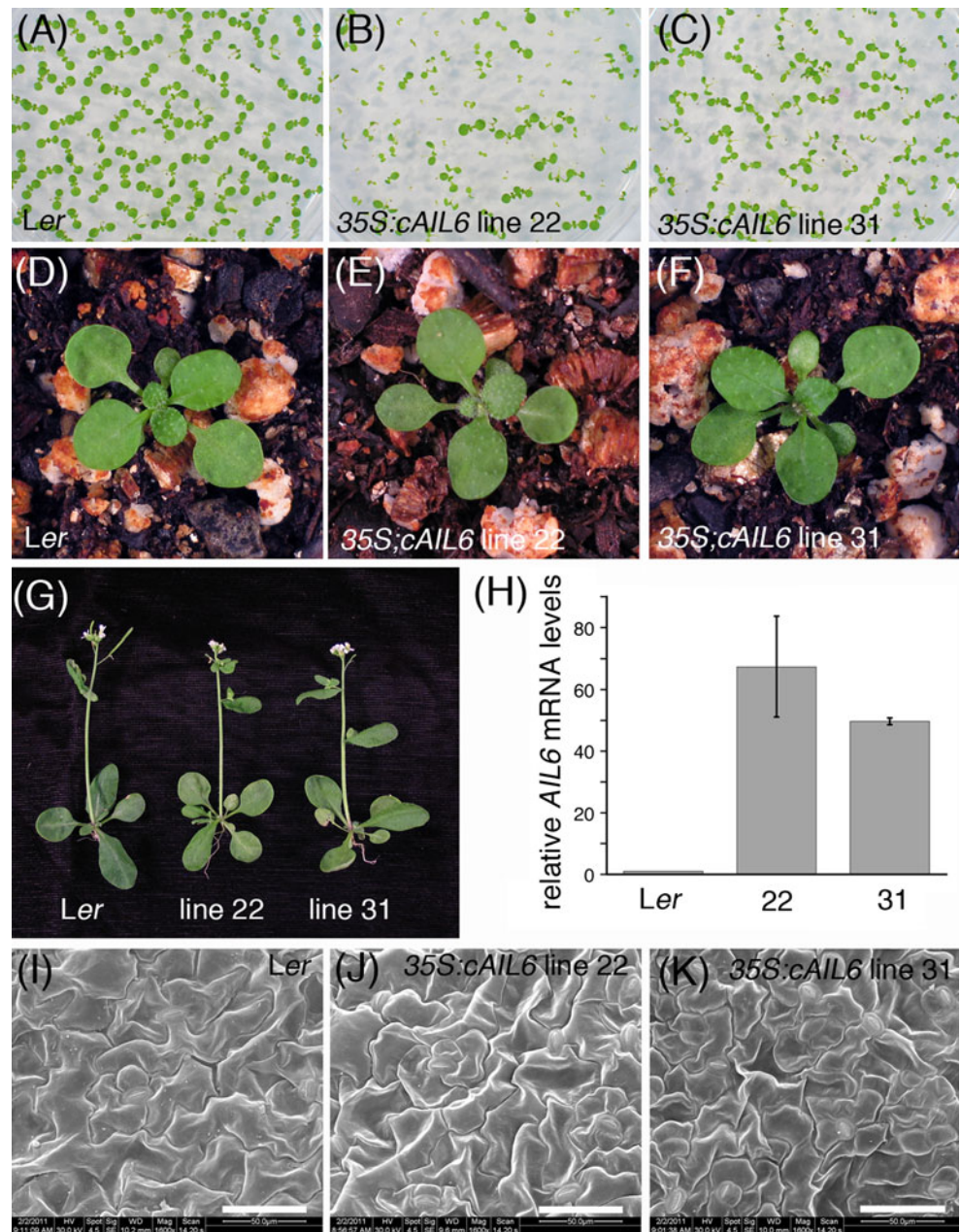
To determine whether the altered size and/or morphology of *35S:cAIL6* floral organs were associated with changes in cell division, we examined the expression pattern of *histone H4* by in situ hybridization. Several obvious differences in *histone H4* expression were observed in *35S:cAIL6* lines. The number of *histone H4* expressing cells was increased in *35S:cAIL6* line 31 stage 10 petals as compared with *Ler* petals of the same age indicating that more cells are dividing in the *35S:cAIL6* petals at this time

in development (Fig. 6a, b). In stage 13 and older flowers, an increased number of *histone H4* expressing cells were detected in the carpel valves and styler region of *35S:cAIL6* line 22 flowers as compared with *Ler* (Fig. 6c–f). These results indicate that ectopic expression of *AIL6* during later stages of flower development promotes cell division in some floral tissues.

35S:cAIL6 lines exhibit uneven *AIL6* expression

Some of the phenotypic effects of *AIL6* overexpression, such as bumps on the surface of sepals and fringe on the distal end of sepals and petals, suggest uneven growth within developing floral organs. To determine whether this might be due to different effects of *AIL6* activity in different cells or unequal accumulation of *AIL6* mRNA, we examined *AIL6* expression in *35S:cAIL6* lines by in situ hybridization. In wild type inflorescences *AIL6* mRNA is detected on the periphery of the inflorescence meristem and in young flowers (Fig. 7a). *AIL6* mRNA is not detected in flowers older than stage 6 (Fig. 7d, h). In *35S:cAIL6* lines, we found that *AIL6* mRNA did not accumulate to similar levels in all tissues even though it is expressed under the control of a constitutive promoter. Although *AIL6* mRNA accumulates unevenly within developing flowers, these expression patterns were consistent among flowers of the same stage. *AIL6* mRNA levels are high in the sepals and pedicels of stage 4–6 *35S:cAIL6* flowers (Fig. 7b, c).

Fig. 5 *AIL6* misexpression does not affect leaf development. *Ler* (a), *35S:cAIL6* line 22 (b) and *35S:cAIL6* line 31 (c) seedlings 7 days after transfer of seeds on plates to growth room. 17 day old *Ler* (d), *35S:cAIL6* line 22 (e), and *35S:cAIL6* line 31 (f) plants. The *35S:cAIL6* and *Ler* plants are of similar size at this stage of development. **g** 30 day old *Ler*, *35S:cAIL6* line 22, *35S:cAIL6* line 31 plants. The *35S:cAIL6* and *Ler* plants bolt at approximately the same time. **h** *AIL6* mRNA levels in 20 day old *Ler* and *35S:cAIL6* (lines 22, and 31) plants. The expression level in *Ler* is set to one and error bars show standard deviation. Scanning electron micrographs of the surface of mature *Ler* (i), *35S:cAIL6* line 22 (j) and *35S:cAIL6* line 31 (k) leaves. Leaf epidermal cell morphology is similar in the *35S:cAIL6* lines and *Ler*. *Size bars* correspond to 50 μ M (i–k)



Starting about stage 8, *AIL6* mRNA was detected in petals and stamens in addition to the sepals and pedicels of *35S:cAIL6* flowers (Fig. 7e, f). Starting about stage 11, *AIL6* mRNA was detected in sepals, petals, stamens and carpels in *35S:cAIL6* flowers and remained especially high in the ovary valves (Fig. 7g) and styler region of mature *35S:cAIL6* line 22 carpels (Fig. 7i, j). *AIL6* expression was generally stronger in stage 13 flowers of line 22 as compared with line 31. The one tissue that we observed somewhat variable *AIL6* expression was sepals of stage 13 flowers. Stage 13 sepals with high levels of *AIL6* mRNA were smaller in size than those with lower *AIL6* expression.

Discussion

AIL6 expression in developing floral organs affects organ size and morphology

Misexpression of *AIL6* in flowers can result in increase growth of floral organs similar to what has been observed in plants in which *ANT* or *AIL5* are constitutively expressed (Krizek 1999; Mizukami and Fischer 2000; Nole-Wilson et al. 2005). However in the case of *35S:cAIL6* plants, organ morphology is also affected, something not observed in *35S:ANT* or *35S:AIL5* flowers. These changes in organ

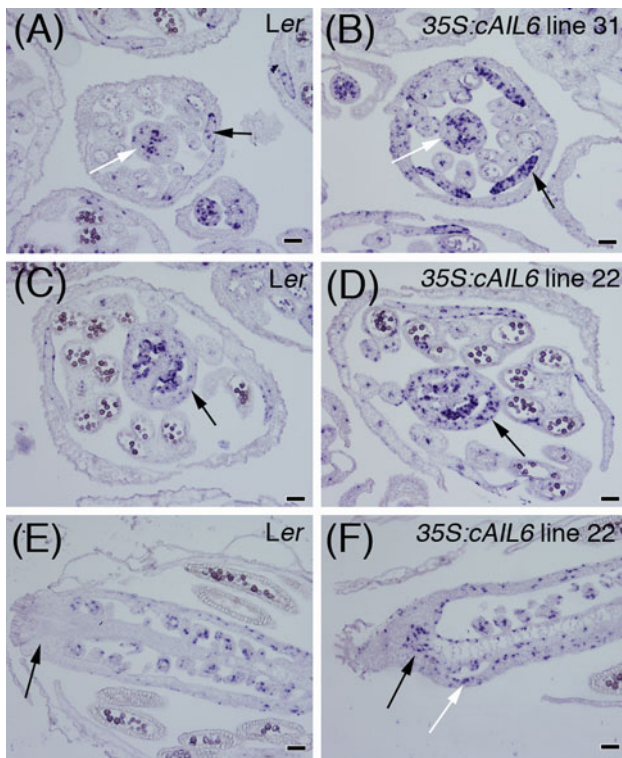


Fig. 6 Extended *histone H4* expression in *35S:cAIL6* floral organs. **a** *Histone H4* expression in a transverse section of a stage 12 *Ler* flower. The white arrow points to the gynoecium and the black arrow points to a petal. **b** Transverse section showing increased numbers of *histone H4* expressing cells in the gynoecium and petals of a *35S:cAIL6* line 31 stage 12 flower. The white arrow points to the gynoecium and the black arrow points to a petal. **c** Transverse section of a stage 13 *Ler* flower. Few cells in the ovary valves (arrow) express *histone H4* at this stage of development. **d** Transverse section of a stage 13 *35S:cAIL6* line 22 flower showing *histone H4* expression in many ovary valves cells (arrow). **e** Longitudinal section of a stage 13 *Ler* flower. No cells in the styler region (arrow) express *histone H4* at this stage of development. **f** Longitudinal section of a stage 13 *35S:cAIL6* line 22 flower showing *histone H4* expression in the styler region (black arrow) and ovary valves (white arrow). Size bars correspond to 50 μ M (a–f)

morphology include bumps or protrusions on sepals and carpels and fringe on the distal end of sepals and petals. The uneven growth and bulging observed in some *35S:cAIL6* floral organs may be a consequence of the uneven accumulation of *AIL6* mRNA within developing floral organs. We observed overlap between cells exhibiting persistent *histone H4* expression and *AIL6* misexpression, suggesting that *AIL6* activity can promote cell proliferation. Patchiness in the distribution of *AIL6* mRNA could lead to uncoordinated cell division within an organ and consequently affect organ morphology.

The different consequences of *ANT* and *AIL6* overexpression suggest that these genes have somewhat distinct functions during flower development. This is consistent with the different expression patterns of these genes; *ANT*

expression is maintained in developing floral organs much longer than *AIL6* (Elliott et al. 1996; Nole-Wilson et al. 2005). In addition, previous work has revealed other differences between *ANT* and *AIL6* suggesting that *AIL6* does not just act similarly to *ANT* in a subset of *ANT* functions within the shoot. For example, *ail6* mutants are more sensitive to the effects of the auxin transport inhibitor NPA on floral meristem initiation than *ant* mutants (Krizek 2011).

High *AIL6* mRNA levels are sufficient to inhibit cell differentiation

We observed somewhat distinct phenotypes in two *35S:cAIL6* lines that accumulated high levels of *AIL6* mRNA. Floral organs of *35S:cAIL6* line 31, which had 30 fold higher *AIL6* mRNA levels as compared with wild type, were increased in size but had fairly normal morphology of sepals, petals and stamens. Cell differentiation occurred normally in this line with epidermal cells of floral organs displaying characteristics of fully differentiated cells. In contrast, floral organs of *35S:cAIL6* line 22, which had 55 fold higher *AIL6* mRNA levels as compared with wild type, exhibited changes in organ morphology and incomplete cell differentiation. Our results suggest that high levels of *AIL6* activity in developing floral organs promotes cell proliferation while extremely high levels of *AIL6* activity can inhibit cell differentiation. These results suggest that *AIL6* regulates both cell proliferation and differentiation and that it can affect cell behaviors in flowers in a dose-dependent manner. The observed premature differentiation of floral meristem cells in *ant ail6* flowers further supports roles for *AIL6* and *ANT* in inhibition of cellular differentiation during early stages of flower development. These functions are consistent with the expression pattern of these genes. While *ANT* expression persists longer than *AIL6* in developing floral organs, neither is expressed in mature organs (Elliott et al. 1996; Nole-Wilson et al. 2005). We hypothesize that changes in the combined *AIL6* and *ANT* activity level regulate the transitioning of cells from a proliferating state toward complete differentiation.

Although *AIL6* mRNA levels in *35S:cAIL6* lines 22 and 31 were higher in leaves as compared with inflorescences, no effect on organ size, morphology or cellular differentiation was observed in the leaves of these plants. This indicates that high *AIL6* activity is not sufficient to promote cell proliferation or inhibit cell differentiation in leaves.

Previous work has suggested that four *AIL/PLT* proteins (*PLT1*, *PLT2*, *AIL6/PLT3* and *BBM*) act in a dosage dependent manner in the root with different levels of overall *PLT* activity specifying distinct cell behaviors along the longitudinal axis of the root (Galinha et al. 2007). Manipulation of this gradient by misexpression of *PLT2*

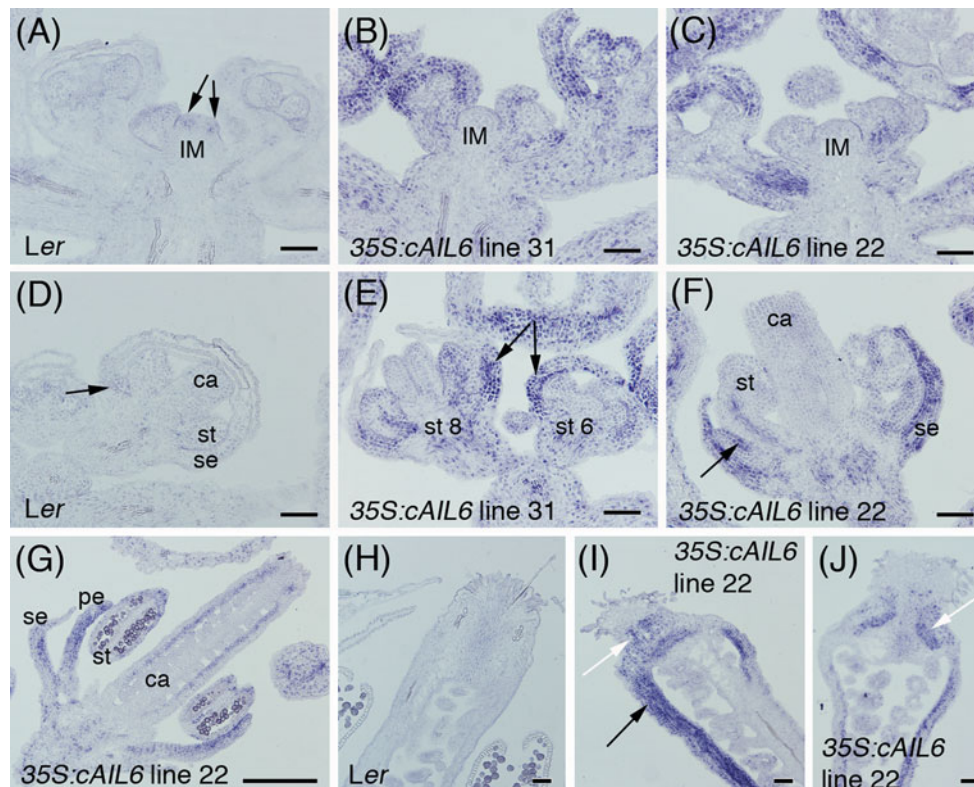


Fig. 7 *AIL6* mRNA does not accumulate evenly in *35S:cAIL6* flowers. **a** *AIL6* mRNA is detected in incipient and young floral primordia (arrows) in *Ler* inflorescences. *AIL6* mRNA accumulates to high levels in some tissues of *35S:cAIL6* line 31 (**b**) and 22 (**c**) inflorescences. **d** *AIL6* is expressed weakly in petal primordia (arrow) in stage 7 *Ler* flowers but is not expressed in later stages of flower development. **e** *AIL6* mRNA accumulates to high levels in the sepals (arrows) of these stage six and eight *35S:cAIL6* line 31 flowers and in the stamens of the stage 8 flower. **f** *AIL6* mRNA in sepals,

petals (arrow) and stamen filaments of a stage ten *35S:cAIL6* line 22 flower. Note that the sepals are reduced in size and do not enclose the floral bud. **g** In stage 13 *35S:cAIL6* line 22 flowers, *AIL6* mRNA is detected in the sepals, petals and in the inner cell layers of the ovary valves. **h** *AIL6* mRNA is not detected in stage 13 *Ler* carpels. **i**, **j** Strong *AIL6* expression is detected in the ovary valves (black arrow) and stylar region (white arrow) of stage 13 *35S:cAIL6* line 22 carpels. *IM* inflorescence meristem, *SE* sepal, *PE* petal, *ST* stamen, *CA* carpel. Size bars correspond to 50 μ M (**a–j**)

under the control of the *35S* promoter resulted in a larger meristem due to continued division of cells that normally would have stopped proliferating and started elongating (Galinha et al. 2007). Our work is consistent with *AIL/PLT* proteins acting in a similar dose-dependent fashion within flowers with different *AIL/PLT* activity levels associated with distinct cellular behaviors.

AIL6 expression under the *35S* promoter led to uneven accumulation of *AIL6* mRNA

Surprisingly, we found that *AIL6* does not accumulate to high levels in all tissues of *35S:cAIL6* inflorescences even though it is expressed under a constitutive promoter. It is possible that the *35S* promoter used in this experiment does not confer constitutive or nearly constitutive expression. Although the *pART7* plasmid containing the *35S* promoter has been commonly used to misexpress genes, we were unable to find published data showing tissue-specific expression resulting from the use of this promoter. Thus, it

is possible that uneven *AIL6* accumulation results from uneven expression of the transgene. Alternatively, *AIL6* may be subject to post-transcriptional regulation. Further work examining the expression of other genes expressed under the control of this *35S* promoter is needed to distinguish between these possibilities.

Acknowledgments We thank Soumitra Ghoshroy and the Electron Microscopy Center staff for advice on the use of the SEM and the ABRC for the F12B17 BAC clone. This work was supported by National Science Foundation (NSF) grant IOS 0922367.

References

- Bechtold N, Ellis J, Pelletier G (1993) In planta *Agrobacterium* mediated gene transfer by infiltration of adult *Arabidopsis thaliana* plants. *CR Acad Sci Ser III Sci Vie* 316:1194–1199
- Breuninger H, Lenhard M (2010) Control of tissue and organ growth in plants. *Curr Top Dev Biol* 91:185–220
- Czechowski T, Stitt M, Altmann T, Udvardi MK, Scheible W-R (2005) Genome-wide identification and testing of superior

- reference genes for transcript normalization in *Arabidopsis*. Plant Physiol 139:5–17
- Elliott RC, Betzner AS, Huttner E, Oakes MP, Tucker WQJ, Gerentes D, Perez P, Smyth DR (1996) *AINTEGUMENTA*, an *APET-ALA2*-like gene of *Arabidopsis* with pleiotropic roles in ovule development and floral organ growth. Plant Cell 8:155–168
- Feng J-X, Liu D, Pan Y, Gong W, Ma L-G, Luo J-C, Deng XW, Zhu Y-X (2005) An annotation update via cDNA sequence analysis and comprehensive profiling of developmental, hormonal or environmental responsiveness of the *Arabidopsis* AP2/EREBP transcription factor gene family. Plant Mol Biol 59:853–868
- Galinha C, Hofhuis H, Luijten M, Willemsen V, Blilou I, Heidstra R, Scheres B (2007) PLETHORA proteins as dose-dependent master regulators of *Arabidopsis* root development. Nature 449:1053–1057
- Irish VF (2010) The flowering of *Arabidopsis* flower development. Plant J 61:1014–1028
- Ito T (2011) Coordination of flower development by homeotic master regulators. Curr Opin Plant Biol 14:53–59
- Kaufmann K, Muino JM, Jauregui R, Airoidi CA, Smaczniak C, Krajewski P, Angenent GC (2009) Targets of the transcription factor SEPALLATA3: integration of developmental and hormonal pathways in the *Arabidopsis* flower. PLoS Biol 7:e1000090
- Kaufmann K, Wellmer F, Muino JM, Ferrier T, Wuest SE, Kumar V, Serrano-Mislata A, Madueno F, Krajewski P, Meyerowitz EM, Angenent GC, Riechmann JL (2010) Orchestration of floral initiation by APETALA1. Science 328:85–89
- Klucher KM, Chow H, Reiser L, Fischer RL (1996) The *AINTEGUMENTA* gene of *Arabidopsis* required for ovule and female gametophyte development is related to the floral homeotic gene *APETALA2*. Plant Cell 8:137–153
- Krizek BA (1999) Ectopic expression of *AINTEGUMENTA* in *Arabidopsis* plants results in increased growth of floral organs. Dev Genet 25:224–236
- Krizek BA (2009) *AINTEGUMENTA* and *AINTEGUMENTA-LIKE6* act redundantly to regulate *Arabidopsis* floral growth and patterning. Plant Physiol 150:1916–1929
- Krizek BA (2011) *Aintegumenta* and *Aintegumenta-Like6* regulate auxin-mediated flower development in *Arabidopsis*. BMC Res Notes 4:176
- Krizek BA, Fletcher JC (2005) Molecular mechanisms of flower development: an armchair guide. Nat Rev Genet 6:688–698
- Melzer R, Theissen G (2009) Reconstitution of ‘floral quartets’ in vitro involving class B and class E floral homeotic proteins. Nucleic Acids Res 37:2723–2736
- Melzer R, Verelst W, Theissen G (2009) The class E floral homeotic protein SEPALLATA3 is sufficient to loop DNA in ‘floral quartets’-like complexes in vitro. Nucleic Acids Res 37:144–157
- Mizukami Y, Fischer RL (2000) Plant organ size control: *AINTEGUMENTA* regulates growth and cell numbers during organogenesis. Proc Natl Acad Sci USA 97:942–947
- Nole-Wilson S, Tranby T, Krizek BA (2005) *AINTEGUMENTA*-like (*AIL*) genes are expressed in young tissues and may specify meristematic or division-competent states. Plant Mol Biol 57: 613–628
- O’Brien TP, Feder N, McCully ME (1964) Polychromatic staining of plant cell walls by toluidine blue O. Protoplasma 59:368–373
- Pfaffl MW (2001) A new mathematical model for relative quantitation in real-time RT-PCR. Nucleic Acids Res 29:2002–2007
- Sablowski R (2010) Genes and functions controlled by floral organ identity genes. Semin Cell Dev Biol 21:94–99
- Sakai WS (1973) Simple method for differential staining of paraffin embedded plant material using toluidine blue O. Stain Technol 48:247–249
- Theissen G (2001) Development of floral organ identity: stories from the MADS house. Curr Opin Plant Biol 4:75–85
- Verwoerd TC, Dekker BMM, Hoekema A (1989) A small scale procedure for the rapid isolation of plant RNAs. Nucleic Acids Res 17:2362
- Zhao S, Fernald RD (2005) Comprehensive algorithm for quantitative real-time polymerase chain reaction. J Comput Biol 12:1045–1062